Biogeosciences
Discussions

1 Glacier loss and vegetation expansion alter organic and inorganic carbon dynamics in alpine
2 streams
3
4 Andrew L. Robison[1], Nicola Deluigi[1], Camille Rolland[1], Nicola Manetti[1], and Tom Battin[1]
5
6 [1]River Ecosystems Laboratory, Center for Alpine and Polar Environmental Research
7 (ALPOLE), Ecole Polytechnique Fédérale de Lausanne (EPFL), Lausanne, Switzerland.
8
9 Corresponding author: Andrew L. Robison, andrew.robison@epfl.ch
10
11 **Abstract**
12 High-mountain ecosystems are experiencing acute effects of climate change, most visibly
13 through glacier recession and the greening of the terrestrial environment. The streams draining
14 these landscapes are affected by these shifts, integrating hydrologic, geologic, and biological
15 signals across the catchment. We examined the organic and inorganic carbon dynamics of
16 streams in four Alpine catchments in Switzerland to assess how glacier loss and vegetation
17 expansion are affecting the carbon cycle of these high mountain ecosystems. We find that
18 organic carbon concentration and fluorescence properties associated with humic-like
19 compounds increase with vegetation cover within a catchment, demonstrating the increasing
20 importance of allochthonous carbon sources following glacier retreat. Meanwhile, streams
21 transitioned from carbon dioxide sinks to sources with decreasing glacier coverage and
22 increased vegetation coverage, with chemical weathering and soil respiration likely determining
23 the balance. Periods of sink behavior were also observed in non-glaciated streams, indicating
24 geochemical consumption of carbon dioxide may be more common in high-mountain,
25 minimally vegetated catchments than previously described. Together, these results demonstrate
26 the dramatic shifts in carbon dynamics of alpine streams following glacier recession, with
27 significant changes to both the organic and inorganic carbon cycles. The clear link between the
28 terrestrial and aquatic zones further emphasizes the coupled dynamics with which all hydrologic
29 and biogeochemical changes in these ecosystems should be considered, including the role of
30 mountain streams in the global carbon cycle.
31
32 **Short summary**
33 Climate change is affecting mountain ecosystems intensely, including the loss of glaciers and
34 the uphill migration of plants. How these changes will affect the streams draining these
35 landscapes is not well known. We sampled streams across a gradient of glacier and vegetation
36 cover in Switzerland and found glacier loss reduced the carbon dioxide sink from weathering,
37 while vegetation cover increased organic carbon in the stream. These changes are important to
38 consider for mountains globally.
39
40 **Keywords**
41 Streams, climate change, glaciers, carbon dioxide, organic carbon
42

1. Introduction

The effects of climate change on high mountain areas are dramatic, with temperatures increasing approximately twice as quickly as in lower elevation areas (IPCC, 2021). With glacial retreat, the streams draining these landscapes are experiencing significant change in the timing, magnitude, and source of flows (Kneib et al., 2020; Mackay et al., 2019). The terrestrial environment is also shifting with the expansion of vegetation spatially (i.e., to higher elevations) and temporally (i.e., longer growing season), both of which have significant hydrologic, biogeochemical, and ecological consequences (Knight and Harrison, 2014; Brighenti et al., 2019). In the Swiss Alps, recent work has highlighted the rapid "greening" of alpine areas and decreasing snow and ice cover (Rumpf et al., 2022). While the implications for terrestrial ecosystems have been examined broadly (Finstad et al., 2016), the impact these changes will exert on the streams draining these landscapes is much less explored (Beniston et al., 2018). Given the global extent and integral role of streams in connecting high mountain areas with downstream ecosystems (Immerzeel et al., 2020), exploring how these landscape alterations will affect the carbon dynamics of streams is critical to contextualize their role in the global cycle (Horgby et al., 2019b).

High mountain streams are tightly linked to the catchment they drain (Milner et al., 2009; Brighenti et al., 2019). In particular, the presence of glaciers dominates stream hydrology (Kneib et al., 2020), with significant geologic, biogeochemical, and ecological implications. For example, as glaciers generally provide a majority of water to their proglacial streams, solute dynamics are frequently controlled by the contents of glacier melt water. For example, dissolved organic carbon (DOC) frozen within glaciers can be the dominant source of DOC to the proglacial stream upon melting (Colombo et al., 2019). The lability of this glacier-derived DOC is often high, serving as a major source of carbon fueling downstream metabolism (Hood et al., 2009). Glaciers are also associated with high rates of geochemical weathering, both below the glacier itself (Anderson et al., 1997) and in the proglacial stream (St. Pierre et al., 2019). The weathering of both carbonate and silicate minerals can consume atmospheric CO_2, whereby CO_2 dissolved in water is converted to bicarbonate through these reactions (Donnini et al., 2016). These reactions involve significant transformations of dissolved inorganic carbon (DIC) and potentially consuming large amounts of carbon dioxide (CO_2) in the process (Hodson et al., 2000).

As glaciers shrink, there is generally a concomitant increase in soil development and vegetation cover within catchments (Guelland et al., 2013; Rumpf et al., 2022). Higher vegetation cover and soil development provides a pool of organic carbon for export to aquatic environments (Garcia et al., 2015). From this change, increases in stream DOC concentration are likely. And indeed, increased DOC in aquatic ecosystems globally has been directly linked to the greening of the terrestrial landscape (Finstad et al., 2016). Elevated aquatic DOC has implications for ecosystem respiration, productivity, and water quality (Roulet and Moore, 2006; Hongve et al., 2004). This change in DOC source also implies changes to the quality of stream organic matter (Zhou et al., 2019), which could further alter stream metabolic regimes by promoting heightened heterotrophy (Bernhardt et al., 2017; Duarte and Prairie, 2005; Boix Canadell et al., 2020). In terms of inorganic carbon, soils frequently represent the dominant source of CO_2 to streams, as the products of soil respiration are transported to the stream via groundwater (Hotchkiss et al., 2015). Thus, as soils develop and allow for the expansion of vegetation in mountain catchments, emissions of CO_2 from the aquatic system may be promoted as the products of soil respiration are transported to the stream and emitted.

Given these complex relationships, consideration of both glacial influence and the terrestrial environment at-large is key to fully contextualize how climate change may alter carbon flows to and from mountain streams. Moreover, both the organic and inorganic carbon components must be evaluated to complete this cycle, providing perspective on the relative

93 influence of different catchment properties. In this study, we aim to evaluate landscape effects
94 on dissolved organic and inorganic carbon dynamics in high mountain streams across a
95 glacial, vegetation, and elevation gradient. By comparing dissolved carbon concentration and
96 fluxes across these gradients, we can directly assess the relative impact of glacial retreat and
97 catchment greening. We hypothesized the presence of glaciers would drive CO_2 consumption
98 (St. Pierre et al., 2019), and the loss of glacier influence would elevate the role of catchment
99 soils as a source of CO_2 (Crawford et al., 2015). We also expected these landscape
100 transformations would shift the dominant source of organic carbon to the stream from the
101 glacier (Colombo et al., 2019) to the terrestrial environment (Fasching et al., 2016), with
102 subsequent changes to the quality of organic matter.
103

104 **2. Methods**
105   Samples of dissolved organic carbon (DOC) and dissolved inorganic carbon (DIC)
106 were collected, as well as *in situ* sensor measurements of dissolved carbon dioxide (pCO_2) in
107 12 streams in the high mountain area of the western Swiss Alps (Figure 1) over five years,
108 2016-2020. The sampling locations covered a broad range of catchment glacier coverage,
109 vegetation coverage, and elevation (Table 1), providing for a space-for-time substitution in
110 which streams draining lower elevation, lower glacier cover, and higher vegetation cover
111 catchments represent potential future conditions of higher elevation, higher glacier cover, and
112 lower vegetation cover catchments. We thus are able to evaluate how these carbon
113 constituents are likely to evolve with ecosystem processes following anthropogenic climate
114 change. Consideration of various other water quality and catchment properties (e.g., dissolved
115 oxygen, inorganic carbon isotopes, dissolved organic matter fluorescence) provides further
116 insight on changes in the relative contribution of geochemical weathering, in-stream
117 processes, and terrestrial inputs within these streams.
118

119 *2.1 Site description*
120   Our 12 stream sampling locations were equally distributed within Vallon de Nant,
121 Champéry, Valsorey and Val Ferret, four catchments in the western Swiss Alps. These sites
122 are part of the METALP project (https://metalp.epfl.ch), which has been described
123 extensively in previous studies (Ulseth et al., 2019; Boix Canadell et al., 2019; Horgby et al.,
124 2019b) and where numerous hydrological and biogeochemical parameters have been
125 monitored since 2016. Among the monitored reaches, seven are glacier-fed, with glacial
126 coverage ranging from 3.41% to 33.5%. The drainage areas vary from 0.31 km^2 to 23.2 km^2,
127 and elevation from 1778 m to 2892 m. Vegetation cover is highest at lower elevations, and
128 ranged from approximately 94% to 21% coverage of the catchment. The geology of
129 Champéry and Vallon de Nant catchments is dominated by carbonate and sedimentary
130 lithology, while that of Valsorey and Val Ferret is characterized by a metamorphic lithology.
131

132

133   Table 1: Catchment names and characteristics.

134

135   Figure 1: Map of the 12 study sites within four catchments of the Alps in southwestern
136   Switzerland.

137

138   *2.2 Grab sampling and sensor measurements*
139   Grab sampling of various physical and chemical parameters were made at all sampling
140   sites at approximately monthly intervals during the snow-free season. These parameters
141   include dissolved organic carbon (DOC), dissolved organic matter (DOM) fluorescence,
142   dissolved nutrients (phosphate, ammonium, nitrate, and nitrite), major ions (sodium,
143   potassium, magnesium, calcium, fluoride, chloride, bromide, and sulfate), the partial pressure
144   of CO_2 (pCO_2), dissolved inorganic carbon (DIC), alkalinity, total suspended solids, and ash-
145   free dry mass. The analysis of these analytes has been described previously (Horgby et al.,
146   2019a; Boix Canadell et al., 2019).
147   Samples for the quantification of DOC and DOM fluorescence are filtered through
148   pre-combusted 0.45 µm GF/F filters (Whatman) into acid-washed and pre-combusted 40 mL
149   amber glass vials. Samples are kept refrigerated and analyzed for concentration within 24 h
150   from collection. DOC was measured using a Sievers M5310C TOC Analyzer (GE Analytical
151   Instruments, New York, USA) while DOM fluorescence excitation-emission matrices (EEMs)
152   were created by measuring fluorescence intensity of samples within a 1 cm cuvette across a
153   range of excitation (240–450 nm, 2 nm increment) and emission (211.19–620.23 nm, 2 nm
154   increments) wavelengths using an Aqualog® optical spectrometer (Horiba, Kyoto, Japan).
155   Absorbance was also measured within a 10 cm cuvette with a Perkin Elmer Lamba 850
156   spectrophotometer (Massachusetts, USA).
157   Samples for the quantification of pCO_2 and the relative stable carbon isotopic
158   composition ($\delta^{13}C$) were collected without filtration in sealed glass vials filled without
159   headspace and analyzed within 24 h from collection. Samples were preprocessed to
160   equilibrate the collected water with synthetic air that is then analyzed with a G2201-i cavity
161   ring-down spectrometer equipped with a Small Sample Isotope Module 2 (CRDS-SSIM2,
162   Picarro Inc., California, USA). Dissolved inorganic carbon (DIC) samples were filtered
163   through 0.2 µm membrane filters into acid-washed 12 mL glass exetainer vials and stored
164   refrigerated until analysis. Two mL of sample were injected into synthetic air-filled, septum
165   capped, 12 mL exetainer vials containing 200 µL 85% phosphoric acid to convert all DIC to
166   gaseous CO_2. The resulting gas phase was then analyzed on the CRDS-SSIM2 and converted
167   into DIC concentration.
168   Additionally, each monitoring station was instrumented with sensors measuring
169   physical and chemical parameters of the water or air at a 10 min frequency, including water
170   temperature, conductivity, turbidity, dissolved oxygen, carbon dioxide (pCO_2), and depth.
171   Specifications, calibration and maintenance procedures of these sensors have been described
172   previously (Horgby et al., 2019b; Boix Canadell et al., 2020). Stream pCO_2 was measured using
173   a CARBOCAP® GMP252 probe (Vaisala, Vantaa, Finland) within a porous
174   polytetrafluoroethylene (ePDFE) semi-permeable membrane. The probes were then protected
175   with a fine-grained mesh, and a metal casing.
176   Discharge was calculated using rating curves relating water depth to discharge (Boix
177   Canadell et al., 2021), where direct measurements of discharge were made using slug
178   injections of sodium chloride (NaCl) as a conservative tracer (Gordon et al., 2004).
179   Additionally, when stream conditions allowed, 10 random measurements of stream depth
180   were collected to provide a measure of average stream morphology to compare with
181   measurements recorded by the sensor installed on the streamside.

182

183 *2.3 CO_2 saturation and efflux*

184   From the 10-minute sensor data, the daily median concentration of CO_2 was found for
185 all sample locations during the monitoring period (Horgby et al., 2019b). The saturation and
186 efflux for these values were then estimated using measurements of stream water temperature,
187 and estimates of barometric pressure, atmospheric concentration of CO_2, and gas exchange
188 velocity. Barometric pressure was obtained from the MeteoSwiss weather station network
189 (Swiss Federal Office and Meteorology and Climatology). The Col du Grand St Bernard
190 station (elevation 2473 m) was used for the Valsorey and Ferret catchments, while the
191 Evionnaz station (482 m) and Les Diablerets (2964 m) stations were used for Champéry and
192 Vallon de Nant stations. Barometric pressure at each monitoring stations (P_{site}, mbar) was
193 adjusted for site-specific elevation and temperature following:

194

195 $$P_{site} = P_0 \exp\left(\frac{-gM(h-h_0)}{RT}\right), \quad (1)$$

196

197 where P_0 (mbar) is the barometric pressure measured at the MeteoSwiss station, h_0 and h (m)
198 are the altitude of the meteorological and at the monitoring stations, respectively, g is the
199 gravity acceleration (9.81 m s^{-2}), M the molar mass of air (0.0289644 kg mol^{-L}) and R the
200 universal gas constant (8.31432 J mol^{-1} K^{-1}). The temperature of air T_{air} (°C) at the METALP
201 stations is estimated through the temperature T_0 (°C) measured at the MeteoSwiss station,
202 where the regional temperature gradient $\Delta T/\Delta h$ is set to -0.54 °C/100 m, obtained from air
203 temperature data collected during the period 1990-2020 by the Evolène-Villa (1427 m) and
204 the Montana (1825 m) weather stations (MeteoSwiss; Deluigi et al., 2017),

205

206 $$T_{air} = T_0 - \left((h-h_0)\cdot\frac{\Delta T}{\Delta h}\right). \quad (2)$$

207

208   Sensor measurements of $p\text{CO}_{2,raw}$ (ppm) were then adjusted to site-specific
209 temperature and barometric pressure following the ideal gas law:

210

211 $$p\text{CO}_{2,corr} = p\text{CO}_{2,raw} \cdot \frac{P_{site}}{1013} \cdot \frac{298}{T_{water}}, \quad (3)$$

212

213 where P_{site} (mbar) is the barometric pressure at each location and T_{water} (K) is the measured
214 water temperature. Dissolved CO_2 concentration ($CO_{2,water}$, μmol L^{-1}) was then derived by
215 multiplying the corrected $p\text{CO}_{2,corr}$ with Henry's constant K_H (mol L^{-1} atm^{-1}) at each site,

216

217 $$CO_{2,water} = p\text{CO}_{2,corr} \cdot K_H. \quad (4)$$

218

219 K_H is a function of the water temperature in Kelvins (T_{water}) with A is 108.3865, B is
220 0.01985076, C is -6919.53, D is -40.4515, E is 669365 according to Plummer and Busenberg
221 (1982),

222

223 $$K_H = 10^{A+B\cdot T_{water}+\frac{C}{T_{water}}+D\cdot\log_{10}(T_{water})+\frac{E}{T_{water}^2}}. \quad (5)$$

224

225 A corresponding dissolved equilibrium concentration of CO_2 ($CO_{2,sat}$, μmol L^{-1}) was
226 calculated for each sensor measurements at each site using an estimate of daily mean
227 atmospheric CO_2 ($CO_{2,air}$),

228 $$CO_{2,sat} = CO_{2,air} \cdot K_H, \quad (6)$$

229
230 by adjusting measurements of CO_2 concentration at Jungfraujoch (freely available at
231 http://www.climate.unibe.ch) for differences in barometric pressure and temperature,
232

233
$$CO_{2,air} = CO_{2,Jungfrau} \cdot \frac{P_{site}}{P_{Jungfraujoch}} \cdot \frac{T_{Jungfraujoch}}{T_{Site}}. \quad (7)$$

234
235 The standard gas transfer velocity (k_{600}, m d^{-1}) was calculated using the relationships
236 developed by Ulseth et al. (2019) and extrapolated from the same 12 streams in this study:
237

238
$$\ln(k_{600}) \text{ for } eD > 0.02 = 1.18 \cdot \ln(eD) + 6.63 \quad (8)$$
239
$$\ln(k_{600}) \text{ for } eD < 0.02 = 0.35 \cdot \ln(eD) + 3.10 \quad (9)$$

240
241 where eD is the stream energy dissipation rate (m^2 s^{-3}), which is obtained by multiplying the
242 gravity acceleration (9.81 m s^{-2}) with slope (S, unitless) and stream flow velocity (V, m s^{-1}),
243

244
$$eD = g \cdot S \cdot V \quad (10)$$

245
246 Velocity was calculated according to the hydraulic geometry scaling proposed by (Horgby et
247 al., 2019b) for these streams,
248

249
$$V = 0.668 \cdot Q^{0.365}, \quad (11)$$

250
251 where Q is discharge (m^3 s^{-1}). To convert k_{600} to k_{CO2} (Eq. 11) we used the temperature
252 dependent Schmidt scaling according to (Wanninkhof, 2014),
253

254
$$Sc_{CO_2} = 1923.6 - 125.06 \cdot T_W + 4.3773 \cdot T_W^2 - 0.85681 \cdot T_W^3 + 0.00070284 \cdot T_W^4 \quad (12)$$

255

256
$$k_{CO_2} = \frac{k_{600}}{\left(\frac{600}{Sc_{CO_2}}\right)^{-0.5}} \quad (13)$$

257
258 The CO_2 efflux (F_{CO2}, g CO_2-C m^{-2} d^{-1}) was then calculated as,
259

260
$$F_{CO_2} = k_{CO_2} \times \left(CO_{2,water} - CO_{2,sat}\right). \quad (14)$$

261
262 *2.4 PARAFAC modelling*
263 Parallel factor analysis (PARAFAC) modelling of fluorescence excitation-emission
264 matrices (EEMs) was used to identify and determine the main fluorescence components of
265 DOM present across collected water samples and was conducted using the R packages
266 *staRdom* (Pucher et al., 2019) and eemR (Massicotte, 2019). Pre-processing of EEMs was
267 necessary prior to PARAFAC development (Murphy et al., 2013; Stedmon & Bro, 2008).
268 Briefly, spectra were corrected for instrument-specific effects, blank subtraction, inner-filter
269 effects. First- and second-order Rayleigh scattering was removed and corrected EEMs
270 normalized to Raman units (Murphy et al., 2010). A total of 220 samples were included for
271 model development. The final PARAFAC model was validated using split-half analysis. The
272 resulting components were compared to previously published fluorescence components from
273 aquatic ecosystems in the OpenFluor database (Murphy et al., 2014).
274

2.5 Statistical analyses

All statistical analyses were performed in MATLAB and Statistics Toolbox Release 2021a (MathWorks, Massachusetts, USA). Differences in concentration or saturation between groups of streams was investigated using Kruskal-Wallis tests. Simple linear regression was used to evaluate relationships between DOC concentration or CO_2 saturation with cacthment properties and water quality parameters. The Pearson correlation coefficient (r) and coefficient of determination (r^2) were used to determine the strength of correlations, with the Pearson correlation coefficient used to show the direction of interaction.

The highly correlated nature of potential explanatory variables limited interpretability for CO_2 saturation, thus we used partial least squares (PLS) regression to identify variables important for predicting median CO_2 saturation at each site. PLS is a method which is well-designed for datasets with many colinear predictor variables and when the number of observations is small relative to the number of predictor variables (Wold et al., 1984; Carrascal et al., 2009; Nash and Chaloud, 2011). Here, our response variable is the median CO_2 saturation of each stream location, and 39 predictor variables (standardized within the PLS model) are included (Table S1).

A Monte-Carlo cross-validation method assessed the predictive ability of the resulting PLS model, where the model was fitted with a sub-sample of data. The calibration validation ratio was set to 0.8, following Onderka et al. (2012), then the resulting fitted models were tested on the validation set. This process was repeated 500 times. The mean cross-validated goodness of prediction (Q^2) was then compared to the original model fit (R^2Y). The strength of each predictor variable within the model was then analyzed using variable importance in the projection (VIP), where highly important variables had $VIP > 1.0$ (Eriksson et al., 2001). Additionally, moderately important ($0.8 < VIP < 1.0$) or less influential ($VIP < 0.8$) variables were identified.

Finally, watershed areal fluxes of CO_2, DIC, and DOC were calculated using watershed area and estimates of stream surface area. We focus on the snow-free period, July 1 through October 31 (Deluigi et al., 2017), to exclude snow cover as a confounding factor affecting gas exchange. Concentration and gas exchange rates are considered constant within subcatchments. An estimation of the network stream area was computed as the product of the stream length and width during this snow free period. Perennial stream length was extracted from the large-scale topographic landscape model of Switzerland (swissTLM3D) and compared to a 2m-resolution DEM stream network (swissALTI3D). Considering the complexity of the network and its remoteness, stream widths were estimated on aerial images with a 25 cm pixel resolution, with a minimum of one width measurement per stream order. An average of 187 width estimates were made per watershed. The catchment area normalized calculation of flux for CO_2 is particularly uncertain as stream surface area (Paillex et al., 2020), gas exchange (Ulseth et al., 2019), and pCO_2 (Horgby et al., 2019a) are each highly dynamic in alpine river networks. Thus, these estimates remain approximations intended to provide perspective on the relative balance of dissolved carbon constituents in these stream networks rather than robust calculations of flux. We consider CO_2 as a vertical flux, either into or out of the stream, while DOC and DIC are downstream fluxes. The downstream DIC flux inherently includes downstream transport of CO_2.

3. Results

3.1 Dissolved carbon concentrations

The overall median concentration of DOC was 222 µg C L^{-1}, with site specific median concentrations ranging from 123 µg C L^{-1} at the upper Val Ferret site (FEU), to 447 in the tributary stream at Vallon de Nant (RIC; Figure 2a; Table 2). All measured DOC

324 concentrations (212 samples) were below 1,000 µg C L^{-1}. From simple linear regression,
325 median DOC concentration at a site varied most strongly with cacthment vegetation cover (r =
326 0.76; Figure 3), δ^{13}C-DIC values (r = -0.75), and catchment glacier cover (r = -0.53).
327

328 Table 2: Median concentration of DOC and DIC, percent saturation of CO_2 and O_2, and
329 isotopic composition of DIC for the 12 sites. Concentration and isotopic composition are
330 summarized from grab samples, while CO_2 and O_2 saturation are summarized from sensor
331 data.

332   Concentrations of DIC were generally greater and more varied than DOC, with an
333 overall median concentration of 1.77 mg C L^{-1} across 191 samples, ranging between 0.79 and
334 2.65 mg C L^{-1} (Figure 2b). DIC concentration was most strongly correlated to decreasing
335 mean catchment elevation (r = -0.67), with the three relatively high elevation Valsorey
336 locations exhibiting significantly lower median concentrations than the other nine sites (p <
337 0.01). The median δ^{13}C-DIC value across sites was -6.14‰ (Table 2). The Champéry
338 locations exhibited the most depleted δ^{13}C-DIC values (median = -9.28‰), which were
339 significantly lower than the remaining nine streams (p = 0.02).
340   Across all streams, the median saturation of CO_2 was 95.1%, with the lowest median
341 saturation of 68.1% measured at the upstream location at Valsorey (VAU) and the highest
342 median saturation of 137% measured at the upstream location at Val Ferret (FEU; Figure 2c).
343 All sites exhibited periods of oversaturation and undersaturation, except for VAU, where
344 undersaturation was always observed. CO_2 saturation was significantly positively correlated
345 with specific conductivity, alkalinity, DIC, and calcium, and negatively correlated with
346 glacier coverage and specific UV absorbance at 254 nm ($SUVA_{254}$). However, the variance
347 explained by any of these individual variables was low ($r^2 < 0.3$). A three-component PLS
348 model was extracted which explained roughly 49% of the variance in median CO_2 saturation
349 ($R^2Y = 0.49$), with moderate predictive power ($Q^2 = 0.42$). Ten variables were deemed highly
350 influential (VIP > 1). These include catchment characteristics of mean elevation, catchment
351 area, glacier cover, and vegetation cover. Additionally, water quality parameters deemed
352 influential were specific conductivity, sulfate and calcium concentration, total suspended
353 solids, and discharge. Additionally, DOC was identified as a moderately influential variable.
354   Dissolved oxygen saturation was much less variable than CO_2 across sites, with
355 median values between 98% and 100% and periods of over- and undersaturation for all sites
356 (Table 2). Similarly, the interquartile range of CO_2 saturation across all sites was large,
357 38.1%, when compared to that of dissolved oxygen, 2.3%.
358

359 Figure 2: Boxplots of a) DOC and b) DIC concentration (mg L^{-1}) from grab samples, and c)
360 CO_2 saturation (%) derived from sensor measurements.
361

362 *3.2 PARAFAC modelling*
363   PARAFAC modelling resulted in a four-component model (Figure S1). In comparing
364 these components to the OpenFluor database, the first (C1) and second component (C2) are
365 likely of terrestrial humic origin, while the third (C3) and fourth (C4) are proteinaceous, likely
366 of microbial origin (Kida et al., 2019). The components resemble those reported from other
367 freshwater and glacial environments (e.g., Spencer et al. 2014, Imbeau and Vincent 2021,
368 Kida et al. 2021). When compared to EEM fluorophore peaks assigned by Coble et al. (1990,
369 1998), C1 appears to reflect the A and C peaks which are associated with humic-like
370 compounds from biodegradation of terrestrial plant matter, while C2 contains peak M, which
371 is linked to humic-like compounds related to primary production. Similarly, C3 appears like

372 the T peak and C4 the B peak, both of which are suggested to be proteinaceous compounds of
373 microbial origin. In general, the humic-associated components were found in greater intensity
374 (median = 0.038 and 0.024 RU for C1 and C2, respectively) than the protein-associated
375 components (median = 0.019 and 0.008 RU for C3 and C4, respectively). Both of the humic-
376 associated components were significantly positively correlated with DOC concentration
377 across all sites, C1 (r = 0.86) and C2 (r = 0.69) (Figure 3). The protein-associated peaks
378 showed little correlation with DOC concentration ($r^2 \leq 0.2$).
379
380 Figure 3: Intensity of the four components within the PARAFAC model against DOC
381 concentration from grab samples, with catchment vegetation cover shown by color. a)
382 Component 1 and b) component 2 represent humic-like compounds while c) component 3 and
383 d) component 4 represent proteinaceous compounds. The coefficient of determination (r^2) is
384 shown for each linear regression.
385
386 *3.3 Watershed carbon fluxes*
387 Total areal fluxes of dissolved carbon during the snow-free period ranged from -0.027
388 to 0.052 g C m^{-2} watershed area d^{-1}, at the upstream Valsorey and downstream Champéry
389 locations, respectively (Figure 4). Considering absolute fluxes, CO_2 was the largest
390 component of the dissolved carbon flux, contributing a median of 67%. DIC contributed 29%
391 to the total carbon flux, and DOC contributed the least (4%). Negative net fluxes of C
392 represent occasions when the stream is estimated to be a net sink of CO_2, and this sink
393 exceeds the downstream transport of DOC and DIC. This occurred in only a single catchment
394 (Valsorey).
395
396 Figure 4: Estimated annual fluxes of the dissolved carbon components (CO_2, DOC, and DIC)
397 normalized for watershed area.
398 **4. Discussion**
399 Comparing the dissolved carbon constituents in stream water within the space-for-time
400 framework provided by these 12 study sites highlights how the changing nature of alpine
401 catchments will have dramatic effects on the stream carbon cycle. There is a clear difference
402 in DOC between higher and lower elevation sites, likely as allochthonous carbon becomes
403 more important with increasing vegetation cover at lower elevation. The saturation of CO_2
404 appears related to these DOC inputs, not only as a potential source of carbon for in-stream
405 respiration, but also as an indicator of an increasing importance of soil-derived CO_2 to the
406 stream. Geochemical weathering remains a significant sink of CO_2, most strongly in glaciated
407 catchments. However, the relevance of geochemical weathering to the CO_2 budget is not
408 limited to glaciated catchments, as periods of under-saturation were observed in non-glaciated
409 streams. The dissolved carbon dynamics of montane streams are thus critically tied to the
410 dissolved carbon dynamics of alpine streams.
411
412 *4.1 Increasing allochthonous DOC in alpine streams*
413 The observed relationships between DOC concentration and catchment vegetation
414 cover, and even more strongly the humic-like components of the DOM pool, suggest
415 allochthonous sources drive the increase in DOC concentration across these alpine streams.
416 Higher stream DOC concentration has been attributed to greater terrestrial inputs and
417 increasing vegetation cover (e.g., Zhou et al. 2019, Pain et al. 2020), as well as decreasing
418 glacier influence (Fellman et al., 2010). The routing of water through catchment soils should
419 thus play an increasingly large role in determining the timing and magnitude of allochthonous
420 carbon export to alpine streams generally. For example, as the terrestrial environment

421 becomes a more important source of DOC to streams, hydrologic transport may become a key
422 limiting process (Boix Canadell et al., 2019). Similarly, rain evens should then be related to
423 increased humic-like DOM inputs from terrestrial sources as transport from hillslope to
424 stream is amplified (Fasching et al., 2016).
425 Vegetation cover, as used in this study, is likely a broad indicator of soil development
426 within the catchment, where accumulation of soil material allows for vegetation expansion
427 (Hagedorn et al., 2019; Henne et al., 2011). The soil then can eventually provide a large pool
428 of organic carbon in glacier forelands for export to the stream (Wietrzyk-Pełka et al., 2020;
429 Dümig et al., 2011). For example, in glacier fed streams in Canada, stream DOC
430 concentration increased with catchment soil development (slope ≈ 0.2 mg C L^{-1} soil %
431 catchment area^{-1}; Lafrenière & Sharp, 2004), similar to our relationship with vegetation (slope
432 $= 0.05$ mg C L^{-1} vegetation % catchment area^{-1}). Either of these metrics, vegetation or soil, are
433 indicative of significant catchment change with implications for terrestrial-aquatic carbon
434 transfers.
435 Considering the greening of the terrestrial environment in the Alps and mountain areas
436 globally (Rumpf et al., 2022), the streams draining these landscapes may be expected to
437 experience an increase in DOC concentration as we have shown here. These changes have
438 important implications for these streams as well as their downstream ecosystems, from
439 altering metabolic regimes by promoting heterotrophy (Hall et al., 2016) to causing higher
440 drinking water production costs (Hongve et al., 2004). This increase in allochthonous DOC is
441 similar to the "browning" observed for many aquatic ecosystems globally (Roulet and Moore,
442 2006; Monteith et al., 2007); however because the chromophoric characteristics of the DOM
443 pool were not quantified in this study, we cannot directly link the increased DOC
444 concentration to browning. Nonetheless, given that browning has frequently been linked to
445 rising concentrations of terrestrially derived DOC, the mechanistic similarities are strong.
446 Impacts specific to browning, such as limiting primary productivity or increasing water
447 temperature (Kritzberg et al., 2019), should also be considered when evaluating the potential
448 implications of increasing DOC concentration in these streams. Even while relatively low in
449 concentration, the foundational physical, biochemical, and ecological nature of DOC within
450 streams magnifies the impact of these changes in DOC concentration and highlight the
451 substantial consequences of vegetation expansion following glacial retreat.
452
453 *4.2 Terrestrial processes drive aquatic CO_2 saturation patterns*
454 With regards to CO_2, extensive periods of undersaturation are relatively rare in
455 riverine systems, but are likely explained by geochemical weathering (St. Pierre et al., 2019).
456 In our study, the isotopic signature of DIC provides the primary evidence of geochemical
457 weathering, where depleted δ^{13}C-DIC values (approximately -9 to -3‰) relative to
458 atmospheric equilibrium are indicative of weathering (Skidmore et al., 2004). This agrees well
459 with glacier-fed streams in Alaska (-7 to 0‰; St. Pierre et al. 2019), and mineral sources of
460 DIC have been highlighted in Swiss alpine streams previously (Horgby et al., 2019b).
461 Furthermore, the PLS model results also distinguish influential factors related to the products
462 of weathering (specific conductivity, sulfate and calcium concentration) or which affect the
463 rate of weathering (glacier cover, runoff, total suspended solids). As such, the role of
464 weathering in consuming CO_2 appears substantial.
465 The importance of geochemical weathering as a CO_2 sink in high mountain areas is
466 well described (Hilton and West, 2020; Donnini et al., 2016), where rapid weathering of
467 carbonate and silicate rock consumes CO_2. In particular, elevated rates of weathering are
468 expected for subglacial environments, where water flows over recently crushed, fine-grained
469 reactive mineral surfaces (Tranter, 2003; Sharp et al., 1995). This process can continue in
470 proglacial streams, where suspended sediments with high surface areas promote continued

471 CO_2 drawdown (St. Pierre et al., 2019). Indeed, we see the lowest CO_2 saturation at the two
472 most glacially influenced streams within the Valsorey catchment, VAU and VAD. Glacially
473 enhanced weathering thus appears significant in this study as well.
474   Still, with periods of CO_2 undersaturation in all our study catchments, geochemical
475 weathering appears to be relevant regardless of the presence of the glacier. To further
476 constrain weathering as the primary sink of CO_2 in these catchments, we can also assess the
477 potential for carbon fixation via photosynthesis as an alternative cause of undersaturation.
478 With oxygen saturation consistently near or below saturation in all streams, photosynthesis is
479 an unlikely driver of CO_2 undersaturation, as oxygen must inherently be above saturation to
480 balance carbon fixation. Productivity has been shown to be limited in these streams outside of
481 small temporal windows of opportunity (Boix Canadell et al., 2021), further reducing the
482 likelihood. Lastly, the lack of variability in oxygen saturation across streams suggests
483 photosynthetic rates do not vary significantly across streams, thus cannot account for the
484 observed variability in CO_2 saturation.
485   In contrast, variability within the DIC isotopic data does help explain the contribution
486 of CO_2 to streams derived from the oxidation of organic matter in the terrestrial environment.
487 The effect of organic carbon oxidation on δ^{13}C-DIC values is depletion, i.e., more negative
488 values (Pawellek and Veizer, 1994). It is thus likely the depleted δ^{13}C-DIC values observed at
489 the Champéry streams are a result of greater rates of organic carbon oxidation, where the pool
490 of organic carbon is evinced by the high vegetation cover and stream DOC concentration. We
491 can more narrowly identify this process as most likely occurring in catchment soils, as the
492 near-equilibrium nature of oxygen and the relatively low concentrations of DOC suggests a
493 minor role for in-stream respiration (Bernhardt et al., 2017). Stream CO_2 is generally
494 supported by external sources of CO_2 such as soil respiration (Hotchkiss et al., 2015;
495 Campeau et al., 2019), and has been shown for mountain streams in particular (Clow et al.,
496 2021; Crawford et al., 2015). Thus, as soils develop and organic carbon accumulates, the
497 potential for terrestrially derived CO_2 inputs to the stream increases and CO_2 saturation
498 increases (Marx et al., 2017).The role of the terrestrial environment in affecting stream CO_2
499 saturation if reinforced by the PLS model, which selected both vegetation cover and DOC
500 concentration as influential variables. As we have shown DOC to be largely terrestrially
501 derived, both of these variables emphasize the role of terrestrial processes in affecting CO_2
502 saturation.
503

504 *4.3 Conceptual model of montane stream carbon budgets*
505   Altogether, these results provide the basis of a simple conceptual model explaining
506 contributions to stream CO_2, thereby explaining saturation dynamics across glacier, soil, and
507 elevation gradients in mountain catchments (Figure 5). Across the entire range of elevation,
508 geochemical weathering acts as a sink of CO_2 (Crawford et al., 2019), where the intensity of
509 this sink is dependent in large part on catchment geology. Where present, glaciers can provide
510 additional weathering potential, whereby higher concentrations of suspended sediment
511 increase mineral surface area greatly (St. Pierre et al., 2019). Moreover, this elevated
512 weathering potential can extend far downstream depending on the suspension and transport of
513 glacial till. Decreasing glacier influence reduces total weathering potential, but CO_2
514 undersaturation as a result of weathering is not limited to glacierized catchments. With the
515 development of soils within the catchment, inputs of allochthonous organic carbon and CO_2
516 increases, elevating CO_2 concentrations. This CO_2 likely derives primarily from soil
517 respiration rather than in-stream respiration of organic carbon (Clow et al., 2021; Singer et al.,
518 2012).
519

520 Figure 5: Conceptual model of processes affecting CO_2 saturation, and thus direction of flux,
521 across glacier, soil, and elevation gradients within montane catchments. Geochemical
522 weathering is important across the entire landscape, but is enhanced under glaciated
523 conditions and nearness to the glacier. As vegetation and soil develop at lower elevation,
524 terrestrial inputs add CO_2 through direct inputs from soil respiration and from organic carbon
525 inputs which fuel in-stream respiration. The net balance of these processes determines the
526 CO_2 saturation. In the aerial picture of the Valsorey catchment, the transition from glacier to
527 vegetation cover can be seen directly.

528

529   Estimated fluxes of dissolved carbon constituents further support this conceptual
530 model and the dominant role of terrestrial processes in determining the relative balance within
531 and between streams. First, the dominance of CO_2 to the absolute total flux emphasizes the
532 significance of gaseous carbon fluxes within river networks (Battin et al., 2023). Differences
533 in CO_2 fluxes across catchments are largely explained by differences in glacier and vegetation
534 cover. Similarly, in a glaciated catchment in Alaska (St. Pierre et al., 2019), the areal rate of
535 CO_2 flux was found to be -0.38 g C m^{-2} catchment area d^{-1}, an order of magnitude higher than
536 our most highly glaciated system (-0.03 g C m^{-2} catchment area d^{-1} at VAU). Following our
537 conceptual model, the difference could be explained by the much more heavily glaciated area
538 of the Alaskan catchment ($> 40\%$). When glacier influence is highest, the potential for
539 weathering is highest as well, driving consumption of CO_2. Yet, even without glacier
540 influence, consumption of CO_2 through weathering is still possible within the catchment and
541 should be considered in montane stream carbon budgets.
542   Across the streams in this study, DOC contributed only 4% to the total carbon flux on
543 average, generally indicating a comparatively small role for organic carbon within the stream.
544 Across the streams, the contribution of DOC to the total carbon flux increases with vegetation
545 cover as well, highlighting the increased role of allochthonous carbon along this gradient. A
546 similar analysis in a boreal catchment in Sweden found DOC accounted for 40% of the total
547 carbon flux on average (Wallin et al., 2013). This elevated contribution reflects a watershed
548 with much greater vegetation cover and soil development. While this supports increased
549 terrestrial contributions of DOC to streams following catchment greening, it also suggests a
550 greater potential for soil respiration and thus transfer of CO_2 to streams as well (Campeau et
551 al., 2019). Thus, the aquatic ecosystem should be increasingly affected by the terrestrial
552 organic carbon pool as vegetation cover expands in montane catchments.
553   Our focus on broad relationships across these 12 locations recognizably conceals how
554 local conditions may affect site specific dynamics. In expanding these analyses to other
555 regions and mountain ranges, more direct geologic perspectives will be needed to differentiate
556 potential geochemical weathering rates (Hilton and West, 2020), and hence the potential for
557 differing CO_2 consumption and solute dynamics. For example, the geological differences
558 across our four catchments imparts unquantified variability within our analysis, such as how
559 the presence of carbonate-containing lithology in the Champéry and Vallon de Nant
560 catchments may promote higher levels of geochemical weathering compared to the
561 metamorphic-dominated Valsorey and Val Ferret. On a finer scale within a stream network,
562 local groundwater inputs can drive CO_2 concentration and emission patterns in streams
563 (Duvert et al., 2018). Thus, monitoring pCO_2 at high spatial intensity may reveal if sampling
564 locations are disproportionately affected by groundwater inflows (Horgby et al., 2019a) or
565 how the transport of glacial till affects geochemical weathering downstream (St. Pierre et al.,
566 2019). Nonetheless, the strength of the observed relationships within our analyses and their
567 consistency with other studies of high mountain streams globally suggest our conceptual
568 model provides a simple, yet important foundation with which to assess carbon dynamics in
569 montane streams.

570 **5. Conclusion**

571   The organic and inorganic components of the dissolved carbon pool shift across a
572 glacier and vegetation gradient, driven by the relative balance of geochemical weathering and
573 terrestrial carbon inputs to the stream. Our results also highlight an expanded importance of
574 geochemical weathering in montane ecosystems globally, whereby carbonate and silicate
575 weathering may consume CO_2 across more mountain landscapes than previously considered
576 (Horgby et al., 2019b). Implications for landscape carbon balances are clear, with decreased
577 potential for CO_2 uptake and increased emissions of terrestrially-derived CO_2 emerging after
578 glacier retreat and landscape greening. The rate of the transition from carbon sink to source is
579 likely accelerated by climate change (Knight and Harrison, 2014), thus continued examination
580 of the contributions of these processes to net stream balances is critical to predicting the future
581 role of mountain catchments in the global carbon cycle.

Biogeosciences Discussions

582 **Data availability**
583 Data used in this analysis is available through the METALP data portal (https://metalp-
584 data.epfl.ch/) or through publicly accessible government portals (e.g.,
585 http://www.climate.unibe.ch)
586
587 **Author contributions**
588 TB secured funding for the research. ND and CR performed field and laboratory analyses.
589 AR, ND, CR, and NM processed and analyzed the results. AR conducted statistical analyses.
590 AR led manuscript development, and revised the manuscript with input from all co-authors.
591
592 **Competing interests**
593 The authors declare that they have no conflict of interest.

594 **Acknowledgements**

600 **References**

601 Anderson, S. P., Drever, J. I., and Humphrey, N. F.: Chemical weathering in glacial
602 environments, Geology, 25, 399–402, https://doi.org/10.1130/0091-
603 7613(1997)025<0399:CWIGE>2.3.CO, 1997.

604 Battin, T. J., Lauerwald, R., Bernhardt, E. S., Bertuzzo, E., Gómez-Gener, L., Hall, R. O.,
605 Hotchkiss, E. R., Maavara, T., Pavelsky, T. M., Ran, L., Raymond, P. A., Rosentreter, J. A.,
606 and Regnier, P.: River ecosystem metabolism and carbon biogeochemistry in a changing
607 world, Nature, 613, 2023.

608 Beniston, M., Farinotti, D., Stoffel, M., Andreassen, L. M., Coppola, E., Eckert, N., Fantini,
609 A., Giacona, F., Hauck, C., Huss, M., Huwald, H., Lehning, M., López-Moreno, J. I.,
610 Magnusson, J., Marty, C., Morán-Tejéda, E., Morin, S., Naaim, M., Provenzale, A., Rabatel,
611 A., Six, D., Stötter, J., Strasser, U., Terzago, S., and Vincent, C.: The European mountain
612 cryosphere: A review of its current state, trends, and future challenges, Cryosphere, 12, 759–
613 794, https://doi.org/10.5194/tc-12-759-2018, 2018.

614 Bernhardt, E. S., Heffernan, J. B., Grimm, N. B., Stanley, E. H., Harvey, J. W., Arroita, M.,
615 Appling, A. P., Cohen, M. J., Mcdowell, W. H., Hall, R. O., Read, J. S., Roberts, B. J., Stets,
616 E. G., and Yackulic, C. B.: The metabolic regimes of flowing waters,
617 https://doi.org/10.1002/lno.10726, 2017.

618 Boix Canadell, M., Escoffier, N., Ulseth, A. J., Lane, S. N., and Battin, T. J.: Alpine glacier
619 shrinkage drives shift in dissolved organic carbon export from quasi-chemostasis to transport
620 limitation, Geophys. Res. Lett., 46, 8872–8881, https://doi.org/10.1029/2019GL083424,
621 2019.

622 Boix Canadell, M., Gómez-Gener, L., Clémençon, M., Lane, S. N., and Battin, T. J.: Daily
623 entropy of dissolved oxygen reveals different energetic regimes and drivers among high-
624 mountain stream types, Limnol. Oceanogr., 1–17, https://doi.org/10.1002/lno.11670, 2020.

625 Boix Canadell, M., Gómez-Gener, L., Ulseth, A. J., Clémençon, M., Lane, S. N., and Battin,
626 T. J.: Regimes of primary production and their drivers in Alpine streams, Freshw. Biol., 66,
627 1449–1463, https://doi.org/10.1111/fwb.13730, 2021.

628 Brighenti, S., Tolotti, M., Bruno, M. C., Wharton, G., Pusch, M. T., and Bertoldi, W.:
629 Ecosystem shifts in Alpine streams under glacier retreat and rock glacier thaw: A review, Sci.
630 Total Environ., 675, 542–559, https://doi.org/10.1016/j.scitotenv.2019.04.221, 2019.

631 Campeau, A., Bishop, K., Amvrosiadi, N., Billett, M. F., Garnett, M. H., Laudon, H., Öquist,
632 M. G., and Wallin, M. B.: Current forest carbon fixation fuels stream CO2 emissions, Nat.
633 Commun., 10, 1–9, https://doi.org/10.1038/s41467-019-09922-3, 2019.

634 Carrascal, L. M., Galván, I., and Gordo, O.: Partial least squares regression as an alternative
635 to current regression methods used in ecology, Oikos, 118, 681–690,
636 https://doi.org/10.1111/j.1600-0706.2008.16881.x, 2009.

637 Clow, D. W., Striegl, R. G., and Dornblaser, M. M.: Spatiotemporal dynamics of CO2 gas
638 exchange from headwater mountain streams, J. Geophys. Res. Biogeosciences, 126, 1–18,
639 https://doi.org/10.1029/2021JG006509, 2021.

640 Coble, P. G., Greent, S. A., Blought, N. V, and Gagosiant, R. B.: Characterization of
641 dissolved organic matter in the Black Sea by fluorescence spectroscopy, Nature, 348, 432–
642 435, https://doi.org/doi/10.1038/348432a0, 1990.

643 Coble, P. G., Castillo, C. E. Del, and Avril, B.: Distribution and optical properties of CDOM
644 in the Arabian Sea during the 1995 Southwest Monsoon, Deep Sea Res. Part II Top. Stud.
645 Oceanogr., 45, 2195–2223, https://doi.org/10.1016/S0967-0645(98)00068-X, 1998.

646 Colombo, N., Bocchiola, D., Martin, M., Confortola, G., Salerno, F., Godone, D., D'Amico,
647 M. E., and Freppaz, M.: High export of nitrogen and dissolved organic carbon from an Alpine
648 glacier (Indren Glacier, NW Italian Alps), Aquat. Sci., 81, 1–13,
649 https://doi.org/10.1007/s00027-019-0670-z, 2019.

650   Crawford, J. T., Dornblaser, M. M., Stanley, E. H., Clow, D. W., and Striegl, R. G.: Source
651   limitation of carbon gas emissions in high-elevation mountain streams and lakes, J. Geophys.
652   Res. Biogeosciences, 120, 952–964, https://doi.org/10.1002/2014JG002861, 2015.
653   Crawford, J. T., Hinckley, E. L. S., Litaor, M. I., Brahney, J., and Neff, J. C.: Evidence for
654   accelerated weathering and sulfate export in high alpine environments, Environ. Res. Lett.,
655   14, https://doi.org/10.1088/1748-9326/ab5d9c, 2019.
656   Deluigi, N., Lambiel, C., and Kanevski, M.: Data-driven mapping of the potential mountain
657   permafrost distribution, Sci. Total Environ., 590–591, 370–380,
658   https://doi.org/10.1016/j.scitotenv.2017.02.041, 2017.
659   Donnini, M., Frondini, F., Probst, J. L., Probst, A., Cardellini, C., Marchesini, I., and
660   Guzzetti, F.: Chemical weathering and consumption of atmospheric carbon dioxide in the
661   Alpine region, Glob. Planet. Change, 136, 65–81,
662   https://doi.org/10.1016/j.gloplacha.2015.10.017, 2016.
663   Duarte, C. M. and Prairie, Y. T.: Prevalence of heterotrophy and atmospheric CO_2 emissions
664   from aquatic ecosystems, Ecosystems, 8, 862–870, https://doi.org/10.1007/s10021-005-0177-
665   4, 2005.
666   Dümig, A., Smittenberg, R., and Kögel-knabner, I.: Concurrent evolution of organic and
667   mineral components during initial soil development after retreat of the Damma glacier ,
668   Switzerland, Geoderma, 163, 83–94, https://doi.org/10.1016/j.geoderma.2011.04.006, 2011.
669   Duvert, C., Butman, D. E., Marx, A., Ribolzi, O., and Hutley, L. B.: CO_2 evasion along
670   streams driven by groundwater inputs and geomorphic controls, Nat. Geosci., 11, 813–818,
671   https://doi.org/10.1038/s41561-018-0245-y, 2018.
672   Eriksson, L., Johansson, E., Kettaneh-Wold, N., and Wold, S.: Multi-and megavariate data
673   analysis: Principles and applications., Umetrics AB, Umeå, Sweden, 2001.
674   Fasching, C., Ulseth, A. J., Schelker, J., Steniczka, G., and Battin, T. J.: Hydrology controls
675   dissolved organic matter export and composition in an Alpine stream and its hyporheic zone,
676   Limnol. Oceanogr., 61, 558–571, https://doi.org/10.1002/lno.10232, 2016.
677   Fellman, J. B., Spencer, R. G. M., Hernes, P. J., Edwards, R. T., D'Amore, D. V., and Hood,
678   E.: The impact of glacier runoff on the biodegradability and biochemical composition of
679   terrigenous dissolved organic matter in near-shore marine ecosystems, Mar. Chem., 121, 112–
680   122, https://doi.org/10.1016/j.marchem.2010.03.009, 2010.
681   Finstad, A. G., Andersen, T., Larsen, S., Tominaga, K., and Blumentrath, S.: From greening
682   to browning: Catchment vegetation development and reduced S-deposition promote organic
683   carbon load on decadal time scales in Nordic lakes, Nat. Publ. Gr., 6, 31944,
684   https://doi.org/10.1038/srep31944, 2016.
685   Garcia, R. D., Reissig, M., Queimaliños, C. P., Garcia, P. E., and Dieguez, M. C.: Climate-
686   driven terrestrial inputs in ultraoligotrophic mountain streams of Andean Patagonia revealed
687   through chromophoric and fluorescent dissolved organic matter, Sci. Total Environ., 521–522,
688   280–292, https://doi.org/10.1016/j.scitotenv.2015.03.102, 2015.
689   Gordon, N. D., McMahon, T. A., Finlayson, B. L., Gippel, C. J., and Nathan, R. J.: Stream
690   hydrology: an introduction for ecologists, John Wiely and Sons, 2004.
691   Guelland, K., Hagedorn, F., Smittenberg, R. H., Goransson, H., Bernasconi, S. M., Hajdas, I.,
692   and Kretzschmar, R.: Evolution of carbon fluxes during initial soil formation along the
693   forefield of Damma glacier, Switzerland, Biogeochemistry, 113, 545–561,
694   https://doi.org/10.1007/s10533-012-9785-1, 2013.
695   Hagedorn, F., Gavazov, K., and Alexander, J. M.: Above- and belowground linkages shape
696   responses of mountain vegetation to climate change, Science (80-.)., 365, 1119–1123,
697   https://doi.org/10.1126/science.aax4737, 2019.
698   Hall, R. O., Tank, J. L., Baker, M. A., Rosi-Marshall, E. J., and Hotchkiss, E. R.: Metabolism,
699   gas exchange, and carbon spiraling in rivers, Ecosystems, 19, 73–86,

700   https://doi.org/10.1007/s10021-015-9918-1, 2016.

701   Henne, P. D., Elkin, C. M., Reineking, B., Bugmann, H., and Tinner, W.: Did soil
702   development limit spruce (Picea abies) expansion in the Central Alps during the Holocene?
703   Testing a palaeobotanical hypothesis with a dynamic landscape model, J. Bio, 38, 933–949,
704   https://doi.org/10.1111/j.1365-2699.2010.02460.x, 2011.

705   Hilton, R. G. and West, A. J.: Mountains, erosion and the carbon cycle, Nat. Rev. Earth
706   Environ., 1, 284–299, https://doi.org/10.1038/s43017-020-0058-6, 2020.

707   Hodson, A., Tranter, M., and Vatne, G.: Contemporary rates of chemical denudation and
708   atmospheric CO2 sequestration in glacier basins: an Arctic perspective, Earth Surf. Process.
709   Landforms, 25, 1447–1471, https://doi.org/10.1002/1096-9837(200012)25:13<1447::AID-
710   ESP156>3.0.CO;2-9, 2000.

711   Hongve, D., Riise, G., and Kristiansen, J. F.: Increased colour and organic acid concentrations
712   in Norwegian forest lakes and drinking water – a result of increased precipitation?, Aquat.
713   Sci., 66, 231–238, https://doi.org/10.1007/s00027-004-0708-7, 2004.

714   Hood, E., Fellman, J., Spencer, R. G. M., Hernes, P. J., Edwards, R., Damore, D., and Scott,
715   D.: Glaciers as a source of ancient and labile organic matter to the marine environment,
716   Nature, 462, 1044–1047, https://doi.org/10.1038/nature08580, 2009.

717   Horgby, Å., Boix Canadell, M., Ulseth, A. J., Vennemann, T. W., and Battin, T. J.: High-
718   resolution spatial sampling identifies groundwater as driver of CO2 dynamics in an alpine
719   stream network, J. Geophys. Res. Biogeosciences, 124, 1961–1976,
720   https://doi.org/10.1029/2019JG005047, 2019a.

721   Horgby, Å., Segatto, P. L., Bertuzzo, E., Lauerwald, R., Lehner, B., Ulseth, A. J.,
722   Vennemann, T. W., and Battin, T. J.: Unexpected large evasion fluxes of carbon dioxide from
723   turbulent streams draining the world's mountains, Nat. Commun., 10,
724   https://doi.org/10.1038/s41467-019-12905-z, 2019b.

725   Hotchkiss, E. R., Hall Jr, R. O., Sponseller, R. A., Butman, D., Klaminder, J., Laudon, H.,
726   Rosvall, M., and Karlsson, J.: Sources of and processes controlling CO2 emissions change
727   with the size of streams and rivers, Nat. Geosci., 8, 696–699,
728   https://doi.org/10.1038/ngeo2507, 2015.

729   Imbeau, E. and Vincent, W. F.: Hidden stores of organic matter in northern lake ice: selective
730   retention of terrestrial particles, phytoplankton and labile carbon, J. Geophys. Res.
731   Biogeosciences, 126, e2020JG006233, https://doi.org/10.1029/2020JG006233, 2021.

732   Immerzeel, W. W., Lutz, A. F., Andrade, M., Bahl, A., Biemans, H., Bolch, T., Hyde, S.,
733   Brumby, S., Davies, B. J., Elmore, A. C., Emmer, A., Feng, M., Fernández, A., Haritashya,
734   U., Kargel, J. S., Koppes, M., Kraaijenbrink, P. D. A., Kulkarni, A. V, Mayewski, P. A.,
735   Pacheco, P., Painter, T. H., Pellicciotti, F., Rajaram, H., Rupper, S., Sinisalo, A., Shrestha, A.
736   B., Viviroli, D., Wada, Y., Xiao, C., Yao, T., and Baillie, J. E. M.: Importance and
737   vulnerability of the world's water towers, Nature, 577, 364–369,
738   https://doi.org/10.1038/s41586-019-1822-y, 2020.

739   Kida, M., Kojima, T., Tanabe, Y., Hayashi, K., Kudoh, S., Maie, N., and Fujitake, N.: Origin,
740   distributions, and environmental significance of ubiquitous humic-like fluorophores in
741   Antarctic lakes and streams, Water Res., 163, 114901,
742   https://doi.org/10.1016/j.watres.2019.114901, 2019.

743   Kida, M., Fujitake, N., Kojima, T., Tanabe, Y., Hayashi, K., Kudoh, S., and Dittmar, T.:
744   Dissolved organic matter processing in pristine Antarctic streams, Environ. Sci. Technol., 55,
745   10175–10185, https://doi.org/10.1021/acs.est.1c03163, 2021.

746   Kneib, M., Cauvy-Fraunié, S., Escoffier, N., Boix Canadell, M., Horgby, and Battin, T. J.:
747   Glacier retreat changes diurnal variation intensity and frequency of hydrologic variables in
748   Alpine and Andean streams, J. Hydrol., 583, 124578,
749   https://doi.org/10.1016/j.jhydrol.2020.124578, 2020.

750   Knight, J. and Harrison, S.: Mountain glacial and paraglacial environments under global
751   climate change: Lessons from the past, future directions and policy implications, Geogr. Ann.
752   Ser. A Phys. Geogr., 96, 245–264, https://doi.org/10.1111/geoa.12051, 2014.
753   Kritzberg, E. S., Hasselquist, E. M., Martin, S., Olsson, O., Stadmark, J., and Valinia, S.:
754   Browning of freshwaters: Consequences to ecosystem services, underlying drivers, and
755   potential mitigation measures, Ambio, 49, 375–390, https://doi.org/10.1007/s13280-019-
756   01227-5, 2019.
757   Lafrenière, M. J. and Sharp, M. J.: The concentration and fluorescence of dissolved organic
758   carbon (DOC) in glacial and nonglacial catchments: interpreting hydrological flow routing
759   and DOC sources, Arctic, Antarct. Alp. Res., 36, 156–165, https://doi.org/10.1657/1523-
760   0430(2004)036[0156:TCAFOD]2.0.CO;2, 2004.
761   Mackay, J. D., Barrand, N. E., Hannah, D. M., Krause, S., Jackson, C. R., Everest, J.,
762   Aoalgeirsdóttir, G., and Black, A.: Future evolution and uncertainty of river flow regime
763   change in a deglaciating river basin, Hydrol. Earth Syst. Sci., 23, 1833–1865,
764   https://doi.org/10.5194/hess-23-1833-2019, 2019.
765   Marx, A., Dusek, J., Jankovec, J., Sanda, M., Vogel, T., van Geldern, R., Hartmann, J., and
766   Barth, J. A. C.: A review of CO_2 and associated carbon dynamics in headwater streams: A
767   global perspective, Rev. Geophys., 55, 560–585, https://doi.org/10.1002/2016RG000547,
768   2017.
769   Massicotte, P.: eemR: tools for pre-processing emission-excitation-matrix (EEM)
770   fluorescence data, R Packag. version 1.0.1, 2019.
771   Masson-Delmotte, V., Zhai, P., Pirani, A., Connors, S. L., Péan, C., Berger, S., Caud, N.,
772   Chen, Y., Goldfarb, L., Gomis, M. I., Huang, M., Leitzell, K., Lonnoy, E., Matthews, J. B. R.,
773   Maycock, T. K., Waterfield, T., Yelekçi, O., Yu, R., and Zhou, B. (Eds.): Climate change
774   2021: The physical science basis. Working Group I contribution to the IPCC Sixth
775   Assessment Report, Cambridge University Press, Cambridge, United Kingdom and New
776   York, NY, USA, https://doi.org/10.1017/9781009157896, 2021.
777   Milner, A. M., Brown, L. E., and Hannah, D. M.: Hydroecological response of river systems
778   to shrinking glaciers, Hydrol. Process., 23, 62–77, https://doi.org/10.1002/hyp, 2009.
779   Monteith, D. T., Stoddard, J. L., Evans, C. D., Wit, H. A. De, Forsius, M., Jeffries, D. S.,
780   Vuorenmaa, J., Keller, B., Wilander, A., and Skjelkva, B. L.: Dissolved organic carbon trends
781   resulting from changes in atmospheric deposition chemistry, 450,
782   https://doi.org/10.1038/nature06316, 2007.
783   Murphy, K. R., Butler, K. D., Spencer, R. G. M., Stedmon, C. A., Boehme, J. R., and Aiken,
784   G. R.: Measurement of dissolved organic matter fluorescence in aquatic environments: an
785   interlaboratory comparison, Environ. Sci. Technol., 44, 9405–9412,
786   https://doi.org/10.1021/es102362t, 2010.
787   Murphy, K. R., Stedmon, C. A., Graeber, D., and Bro, R.: Fluorescence spectroscopy and
788   multi-way techniques. PARAFAC, Anal. Methods, 5, 6557,
789   https://doi.org/10.1039/c3ay41160e, 2013.
790   Murphy, K. R., Stedmon, C. A., Wenig, P., and Bro, R.: OpenFluor – an online spectral
791   library of auto- fl uorescence by organic compounds in the environment †, Anal. Methods, 6,
792   658–661, https://doi.org/10.1039/c3ay41935e, 2014.
793   Nash, M. S. and Chaloud, D. J.: Partial least square analyses of landscape and surface water
794   biota sssociations in the Savannah River basin, ISRN Ecol., 2011, 1–11,
795   https://doi.org/10.5402/2011/571749, 2011.
796   Onderka, M., Wrede, S., Rodný, M., Pfister, L., Hoffmann, L., and Krein, A.: Hydrogeologic
797   and landscape controls of dissolved inorganic nitrogen (DIN) and dissolved silica (DSi) fluxes
798   in heterogeneous catchments, J. Hydrol., 450–451, 36–47,
799   https://doi.org/10.1016/j.jhydrol.2012.05.035, 2012.

800 Paillex, A., Siebers, A. R., Ebi, C., Mesman, J., and Robinson, C. T.: High stream
801 intermittency in an alpine fluvial network: Val Roseg, Switzerland, Limnol. Oceanogr., 65,
802 557–568, https://doi.org/10.1002/lno.11324, 2020.
803 Pain, A. J., Martin, J. B., Martin, E. E., Rahman, S., and Ackermann, P.: Differences in the
804 quantity and quality of organic matter exported from Greenlandic glacial and deglaciated
805 watersheds, Global Biogeochem. Cycles, 34, 1–20, https://doi.org/10.1029/2020GB006614,
806 2020.
807 Pawellek, F. and Veizer, J.: Carbon cycle in the upper Danube and its tributaries: δ13C-DIC
808 constraints, Isr. J. Earth Sci., 43, 187–194, 1994.
809 St. Pierre, K. A., St. Louis, V. L., Schiff, S. L., Lehnherr, I., Dainard, P. G., Gardner, A. S.,
810 Aukes, P. J. K., and Sharp, M. J.: Proglacial freshwaters are significant and previously
811 unrecognized sinks of atmospheric CO_2, Proc. Natl. Acad. Sci. U. S. A., 116, 17690–17695,
812 https://doi.org/10.1073/pnas.1904241116, 2019.
813 Plummer, L. N. and Busenberg, E.: The solubilities of calcite, aragonite and vaterite in CO_2-
814 H_2O solutions between 0 and 90°C, and an evaluation of the aqueous model for the system
815 $CaCO_3$-CO_2-H_2O, Geochim. Cosmochim. Acta, 46, 1011–1040,
816 https://doi.org/10.1016/0016-7037(82)90056-4, 1982.
817 Pucher, M., Wünsch, U., Weigelhofer, G., Murphy, K., Hein, T., and Graeber, D.: staRdom:
818 versatile software for analyzing spectroscopic data of dissolved organic matter in R, Water,
819 11, 2366, https://doi.org/10.3390/w11112366, 2019.
820 Rehn, L., Sponseller, R. A., Laudon, H., and Wallin, M. B.: Long-term changes in dissolved
821 inorganic carbon across boreal streams caused by altered hydrology, Limnol. Oceanogr., 1–
822 15, https://doi.org/10.1002/lno.12282, 2022.
823 Roulet, N. and Moore, T. R.: Browning the waters, Nature, 444, 283–284,
824 https://doi.org/10.1038/444283a, 2006.
825 Rumpf, S. B., Gravey, M., Brönnimann, O., Luoto, M., Cianfrani, C., Mariethoz, G., and
826 Guisan, A.: From white to green: Snow cover loss and increased vegetation productivity in
827 the European Alps, Science (80-.)., 1122, 1119–1122, 2022.
828 Sharp, M., Tranter, M., Brown, G. H., and Skidmore, M.: Rates of chemical denudation and
829 CO_2 drawdown in a glacier-covered alpine catchment, Geology, 23, 61–64,
830 https://doi.org/10.1130/0091-7613(1995)023<0061:ROCDAC>2.3.CO;2, 1995.
831 Singer, G. A., Fasching, C., Wilhelm, L., Niggemann, J., Steier, P., Dittmar, T., and Battin, T.
832 J.: Biogeochemically diverse organic matter in Alpine glaciers and its downstream fate, Nat.
833 Geosci., 5, 710–714, https://doi.org/10.1038/ngeo1581, 2012.
834 Skidmore, M., Sharp, M., and Tranter, M.: Kinetic isotopic fractionation during carbonate
835 dissolution in laboratory experiments : implications for detection of microbial CO_2 signatures
836 using □ 13 C-DIC, Geochim. Cosmochim. Acta, 68, 4309–4317,
837 https://doi.org/10.1016/j.gca.2003.09.024, 2004.
838 Spencer, R. G. M., Vermilyea, A., Fellman, J., Raymond, P., Stubbins, A., Scott, D., and
839 Hood, E.: Seasonal variability of organic matter composition in an Alaskan glacier out flow:
840 insights into glacier carbon sources, Environ. Res. Lett., 9, 055005,
841 https://doi.org/10.1088/1748-9326/9/5/055005, 2014.
842 Stedmon, C. A. and Bro, R.: Characterizing dissolved organic matter fluorescence with
843 parallel factor analysis: a tutorial, Limnol. Oceanogr. Fluids Environ., 6, 572–579,
844 https://doi.org/10.4319/lom.2008.6.572, 2008.
845 Tranter, M.: Geochemical weathering in glacial and proglacial environments, Treatise on
846 Geochemistry, 5, 605, https://doi.org/10.1016/B0-08-043751-6/05078-7, 2003.
847 Ulseth, A. J., Hall, R. O., Boix Canadell, M., Madinger, H. L., Niayifar, A., and Battin, T. J.:
848 Distinct air–water gas exchange regimes in low- and high-energy streams, Nat. Geosci., 12,
849 259–263, https://doi.org/10.1038/s41561-019-0324-8, 2019.

850   Wallin, M. B., Grabs, T., Buffam, I., Laudon, H., Ågren, A., Öquist, M. G., and Bishop, K.:
851   Evasion of CO2 from streams - The dominant component of the carbon export through the
852   aquatic conduit in a boreal landscape, Glob. Chang. Biol., 19, 785–797,
853   https://doi.org/10.1111/gcb.12083, 2013.
854   Wanninkhof, R.: Relationship between wind speed and gas exchange over the ocean revisited,
855   Limnol. Oceanogr. Methods, 12, 351–362, https://doi.org/10.4319/lom.2014.12.351, 2014.
856   Wietrzyk-Pełka, P., Rola, K., Szymański, W., and Węgrzyn, M. H.: Organic carbon
857   accumulation in the glacier forelands with regard to variability of environmental conditions in
858   different ecogenesis stages of High Arctic ecosystems, Sci. Total Environ., 717, 1–12,
859   https://doi.org/10.1016/j.scitotenv.2019.135151, 2020.
860   Wold, S., Ruhe, A., Wold, H., and Dunn III, W. J.: The collinearity problem in linear
861   regression. The partial least squares (PLS) approach to generalized inverses, SIAM J. Sci.
862   Stat. Comput., 5, 735–743, 1984.
863   Zhou, Y., Zhou, L., He, X., Jang, K. S., Yao, X., Hu, Y., Zhang, Y., Li, X., Spencer, R. G. M.,
864   Brookes, J. D., and Jeppesen, E.: Variability in dissolved organic matter composition and
865   biolability across gradients of glacial coverage and distance from glacial terminus on the
866   Tibetan Plateau, Environ. Sci. Technol., 53, 12207–12217,
867   https://doi.org/10.1021/acs.est.9b03348, 2019.
868

869 **Tables**

870 Table 1: Catchment names and characteristics.

| Catchment	ID	Station	Altitude (m)	Area (km^2)	Glacier coverage (%)	Vegetation coverage (%)	Geology
Valsorey	VAD	Down	1936	23.2	27.4	24.2	
	VAU	Up	2148	18.1	33.5	21.1	
	VEL	Tributary	2161	3.11	0	56.7	
Ferret	FED	Down	1773	20.2	3.41	62.4	
	FEU	Up	1996	9.33	7.40	46.3	
	PEU	Tributary	2024	3.97	0	70.2	
Vallon de Nant	AND	Down	1197	13.4	4.58	63.9	
	AVU	Up	1465	8.99	6.80	54.0	
	RIC	Tributary	1192	14.3	6.38	64.2	
Champery	VID	Down	1416	3.64	0	94.0	
	VIM	Middle	1630	0.74	0	86.1	
	VIU	Up	1689	0.31	0	80.9	

871

21

872 Table 2: Median concentration of DOC and DIC, percent saturation of CO_2 and O_2, and
873 isotopic composition of DIC for the 12 sites. Concentration and isotopic composition are
874 summarized from grab samples, while CO_2 and O_2 saturation are summarized from sensor
875 data.

Catchment	Station	DOC (μg L^{-1})	DIC (mg L^{-1})	$CO_{2,sat}$ (%)	$O_{2,sat}$ (%)	δ^{13}C-DIC (‰)
Valsorey	Down	189	0.79	77.4	98.6	-5.34
	Up	167	0.80	68,1	99.0	-6.08
	Tributary	304	0.84	77.7	98.3	-6.57
Ferret	Down	176	1.82	90.7	99.3	-4.04
	Up	123	1.38	137	99.0	-3.98
	Tributary	150	1.93	97.0	99.5	-3.67
Vallon de Nant	Down	143	1.76	98.4	99.8	-5.10
	Up	127	1.79	123	99.0	-6.31
	Tributary	447	2.01	100	99.2	-6.96
Champery	Down	363	2.65	130	99.2	-8.45
	Middle	381	2.22	103	99.5	-9.29
	Up	309	2.13	96.2	98.8	-9.76

876
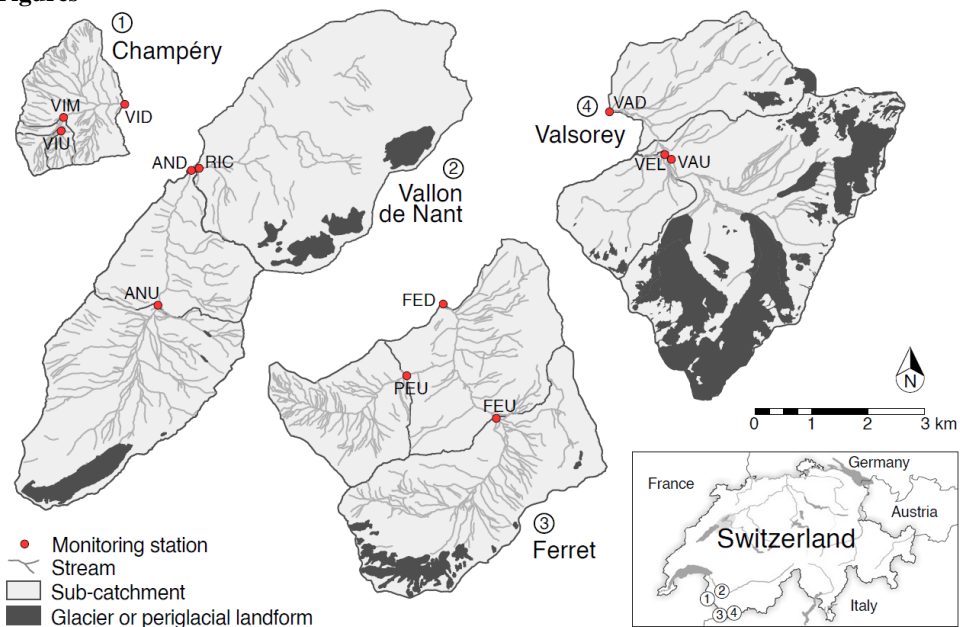
Figures
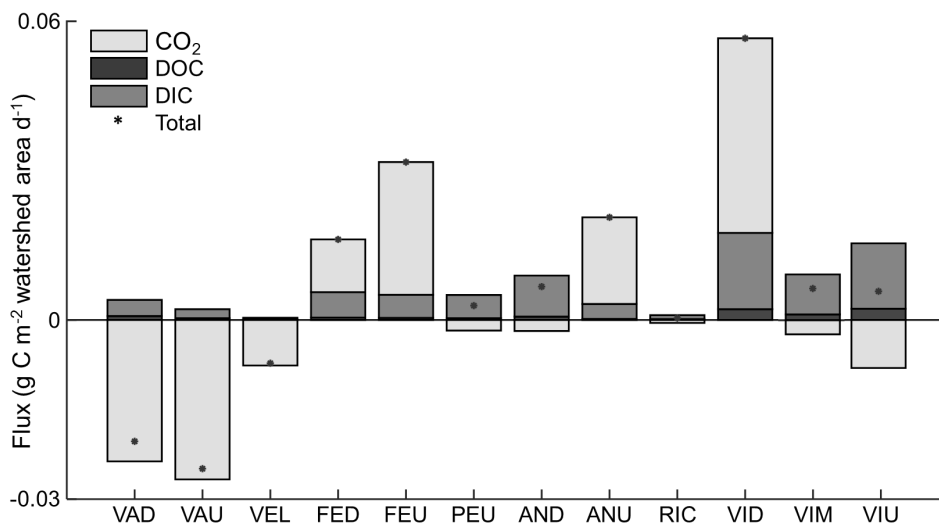

Figure 1: Map of the 12 study sites within four catchments of the Alps in southwestern Switzerland.
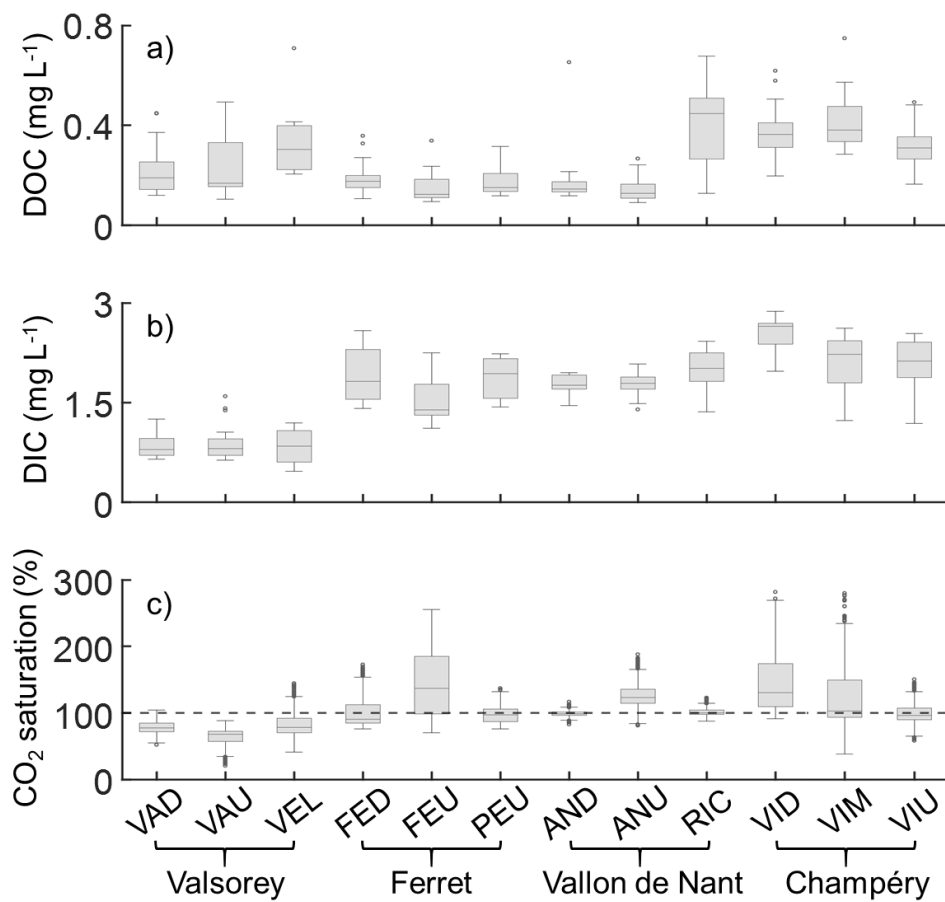
Figure 2: Boxplots of a) DOC and b) DIC concentration (mg L^{-1}) from grab samples, and c) CO$_2$ saturation (%) derived from sensor measurements.
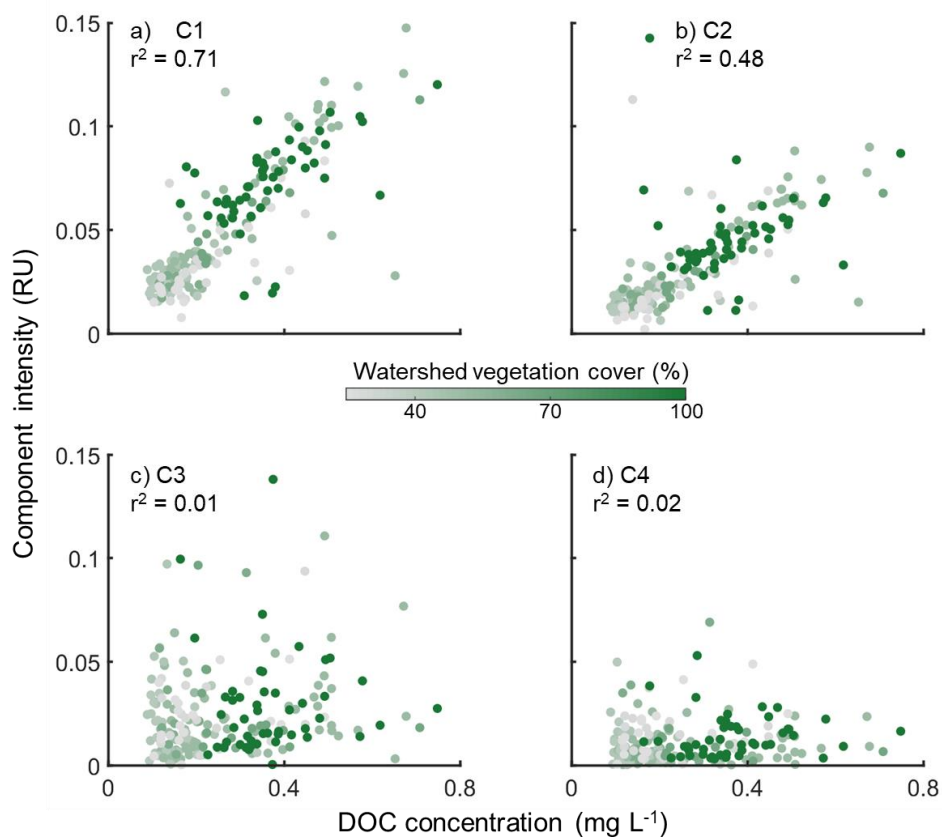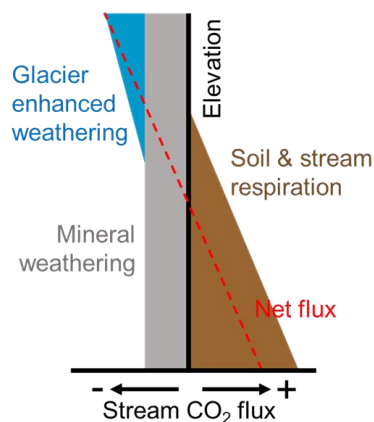
884
885 Figure 3: Intensity of the four components within the PARAFAC model against DOC
886 concentration from grab samples, with catchment vegetation cover shown by color. a)
887 Component 1 and b) component 2 represent humic-like compounds while c) component 3 and
888 d) component 4 represent proteinaceous compounds. The coefficient of determination (r^2) is
889 shown for each linear regression.

890
891 Figure 4: Estimated annual fluxes of the dissolved carbon components (CO_2, DOC, and DIC)
892 normalized for watershed area.

Biogeosciences
Discussions
Open Access
EGU

893
Figure 5: Conceptual model of processes affecting CO_2 saturation, and thus direction of flux,
across glacier, soil, and elevation gradients within montane catchments. Geochemical
weathering is important across the entire landscape, but is enhanced under glaciated
conditions and nearness to the glacier. As vegetation and soil develop at lower elevation,
terrestrial inputs add CO_2 through direct inputs from soil respiraton and from organic carbon
inputs which fuel in-stream respiration. The net balance of these processes determines the
CO_2 saturation. In the aerial image of the Valsorey catchment, the transition from glacier to
vegetation influence can be seen directly (from Google Earth 2023).